Magmatic Underplating, Extension, and Crustal Reequilibration: Insights from a Cross-Section through the Ivrea Zone and Strona-Ceneri Zone, Northern Italy[1]

Andreas Henk, Leander Franz,[2] *Stefan Teufel,*[2,3] *and Onno Oncken*[2]
Universität Würzburg, Pleicherwall 1, D-97070 Würzburg, Germany

ABSTRACT

The thermal impact of magmatic underplating at various crustal levels is studied along a traverse through the Ivrea-Verbano Zone and Strona-Ceneri Zone in northern Italy. Geochronological and petrologic data are compared to a two-dimensional thermal-kinematic model. Field data and numerical simulation show the strong disturbance of the temperature field in the lower and intermediate crust in relation to magmatic underplating leading to granulite- to amphibolite-facies metamorphism as well as reequilibration of mineral chemical and isotopic systems. Magmatic underplating leaves a crust with an apparently heterogeneous tectonometamorphic evolution, as information on the earlier history is preserved only at upper crustal levels.

Introduction

Because of the relatively low densities of crustal rocks, basaltic magmas generated beneath continental areas are frequently emplaced at the Moho and in the lowermost crust. This process of magmatic underplating adds mass and heat to the continental crust and can cause, among other effects, regional-scale granulite- to amphibolite-facies metamorphism, anatexis, and surface uplift (Huppert and Sparks 1988; Fountain 1989; Mareschal and Bergantz 1990). We focus on the intense disturbance of the crustal temperature field in relation to magmatic underplating. Depending on the amount of heat gained from cooling and crystallization of the mafic intrusions, metamorphic textures as well as chemical and isotopic equilibria in the lower and intermediate crust may be largely reset.

Most metamorphic terranes cannot reveal the complex depth-dependent effects of magmatic underplating, since usually only a certain crustal and metamorphic level is exposed. The Ivrea-Verbano Zone and Strona-Ceneri Zone in northwestern Italy provide one of the rare opportunities in the world to study a coherent crustal succession from the Moho to upper crustal levels. The Ivrea Zone achieved its present structure largely at the end of and shortly after the Hercynian orogeny. It therefore also presents a prime opportunity for investigating late- to post-orogenic crustal reequilibration and its relation to magmatism in general. We chose this classical cross-section to compare new geochronological and petrologic data with predictions from a two-dimensional thermal-kinematic model. Modeling results are expected to provide insights in the variable but contemporaneous metamorphic evolution at different crustal levels and the interplay between deformation and metamorphism during magmatic underplating and crustal attenuation.

Geological Setting and General Evolution of the Study Area

The Ivrea-Verbano Zone (IVZ) and adjacent Strona-Ceneri Zone (SCZ) in northern Italy are part of the pre-Alpine basement of the southern Alps (see Boriani et al. 1990*a,* 1990*b;* Zingg et al. 1990; Handy and Zingg 1991; Schmid 1993). The two zones form a SW-NE striking crustal segment exposed over 130 km length and 10–50 km width (figure 1). Bounded to the northwest by the Insubric Line (IL), the IVZ

[1] Manuscript received August 5, 1996; accepted December 3, 1996.

[2] GeoForschungsZentrum, Telegrafenberg, D-14473 Potsdam, Germany.

[3] Deceased.

[The Journal of Geology, 1997, volume 105, p. 000–000] 0022-1376/97/10503-0006$01.00

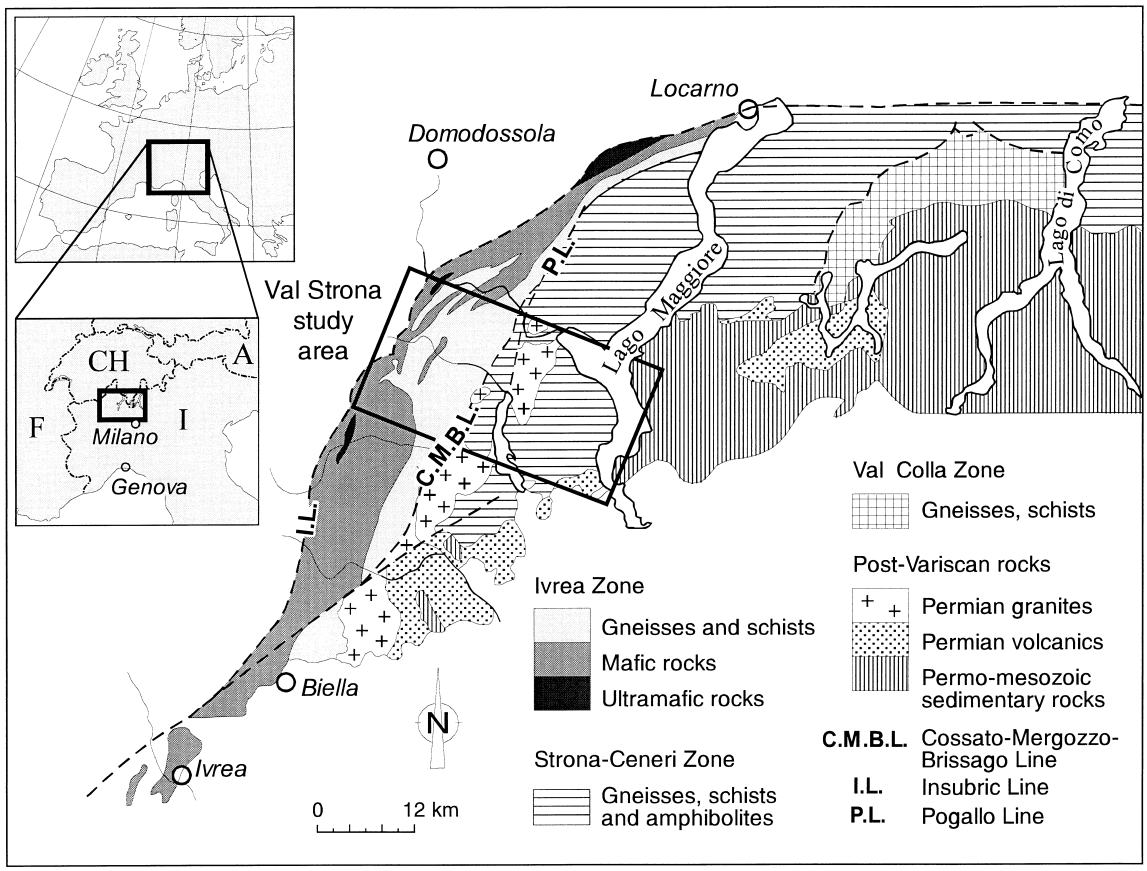

Figure 1. Geological map of the Ivrea Zone and Strona-Ceneri Zone (simplified after Zingg et. al. 1990) showing modeled crustal segment (box) centered around the Val Strona.

displays a continuous succession through thinned lower to intermediate continental crust. The base is formed by metagabbros, ultramafic bodies, and diorites of the so-called Mafic Formation. They intruded into a sequence of metapelites, -psammites, -basites and minor marbles, locally called the Kinzigite Formation. The SCZ is regarded as the—possibly decoupled—upper crust of the IVZ. It displays a series of interlayered metasedimentary rocks, orthogneisses and minor amphibolites intruded by late Paleozoic granites. Farther to the east, the metamorphic basement rocks of the SCZ are overlain by Permo-Carboniferous sedimentary and volcanic rocks as well as by Mesozoic rift basins and shelf sequences. IVZ and SCZ are separated by the Pogallo Line (PL), which has been interpreted as a major tilted normal fault zone (Hodges and Fountain 1984; Handy 1987), and the Cossato-Mergozzo-Brissago Line (CMBL; Boriani et al. 1990*a*).

The study presented here concentrates on the post-Hercynian, i.e., Late Carboniferous to Early Permian, evolution of the IVZ and SCZ. An earlier cycle of metamorphism and deformation started in the late Proterozoic or early Paleozoic and lasted until the end of the Hercynian orogeny (>300 Ma; Schmid 1993). Remnants of the related pressure-dominated metamorphism are mainly preserved in the SCZ (Borghi 1988; Schmid 1993). The IVZ achieved most of its present compositional and metamorphic zonation after the Hercynian orogeny when a normal crustal thickness of about 30 km was already established (Handy and Zingg 1991). During the Late Paleozoic, large volumes of mafic magmas were emplaced at or near the Moho, resulting in high-temperature metamorphism and partial melting of lower crustal rocks (Voshage et al. 1990; Sinigoi et al. 1994). Earlier Sm-Nd data of Voshage et al. (1987) seemed to indicate a Mafic Formation age of about 600 Ma, but reinterpretation of this data set (Voshage et al. 1990) supports a late Paleozoic formation age. This agrees with SHRIMP data on Ivrea Zone zircons by Vavra et al. (1996). Handy and Zingg (1991) propose that a new stress field established during very Late Carboniferous to Early Permian times resulted in local sinistral transtension. A second episode of crustal attenuation, ultimately leading to passive continental

margin formation, occurred between the Late Triassic and the Middle Jurassic. During Alpine evolution, IVZ and SCZ were affected mainly by brittle to semi-brittle deformation under greenschist-facies metamorphic conditions. Tilting of the IVZ to its present, almost vertical position probably occurred during Late Oligocene to Early Miocene times (Handy 1987; Schmid 1993).

Constraints for Permo-Carboniferous Tectonometamorphic Evolution

Samples for geochronological and petrologic studies were collected systematically along a traverse across strike of the IVZ and SCZ along the Val Strona (figure 2). As the IVZ is presently in a nearly upright position; this part of the traverse forms a continuous cross-section exposing true thicknesses.

Petrology and Thermobarometry. Petrological investigations in the Val Strona were already performed by Sills (1984), who described granulite-facies metamorphism with maximum P-T-conditions of 750 ± 50°C and 6 ± 1 kbar in metapelites from the NW part of the valley. Thermometric investigations using the calcite-carbon-isotope method yielded elevated temperatures of 750–800°C at the base of the granulitic complex and temperatures of <600°C near Omegna (Strackenbrock-Gehrke 1989). For petrological and thermobarometric investigations, 10 representative samples of metapelites and metabasites were investigated with the electron microprobe. The sample locations, petrographic rock descriptions, P-T estimates, and applied thermobarometric methods are summarized in table 1. A compilation of the mineral-chemical data used to estimate the metamorphic conditions can be found in the data depository to this article, available from *The Journal of Geology* upon request.

Our petrologic studies (figure 2, bottom) show the highest metamorphic P-T-conditions for a metagabbro from the base of the Mafic Formation, close to the IL (sample IZ-93-60). Its mineral assemblage is Grt-Cpx-Pl-Rt-Ilm ± Opx (mineral abbreviations following Kretz 1983). Clinopyroxene inclusions in the garnet core reveal temperatures of 770–780°C using the calibration of Ellis and Green (1979) (also reproduced by Berman et al. 1995). This is in accordance with temperatures of about 800°C determined with the method of Lal (1993) using the Fe/Mg-exchange of garnet cores and relictic orthopyroxene. Due to the absence of quartz, a precise geobarometry within these samples is problematic. Maximum pressures of 7.8–8.6 kbar can be esti-

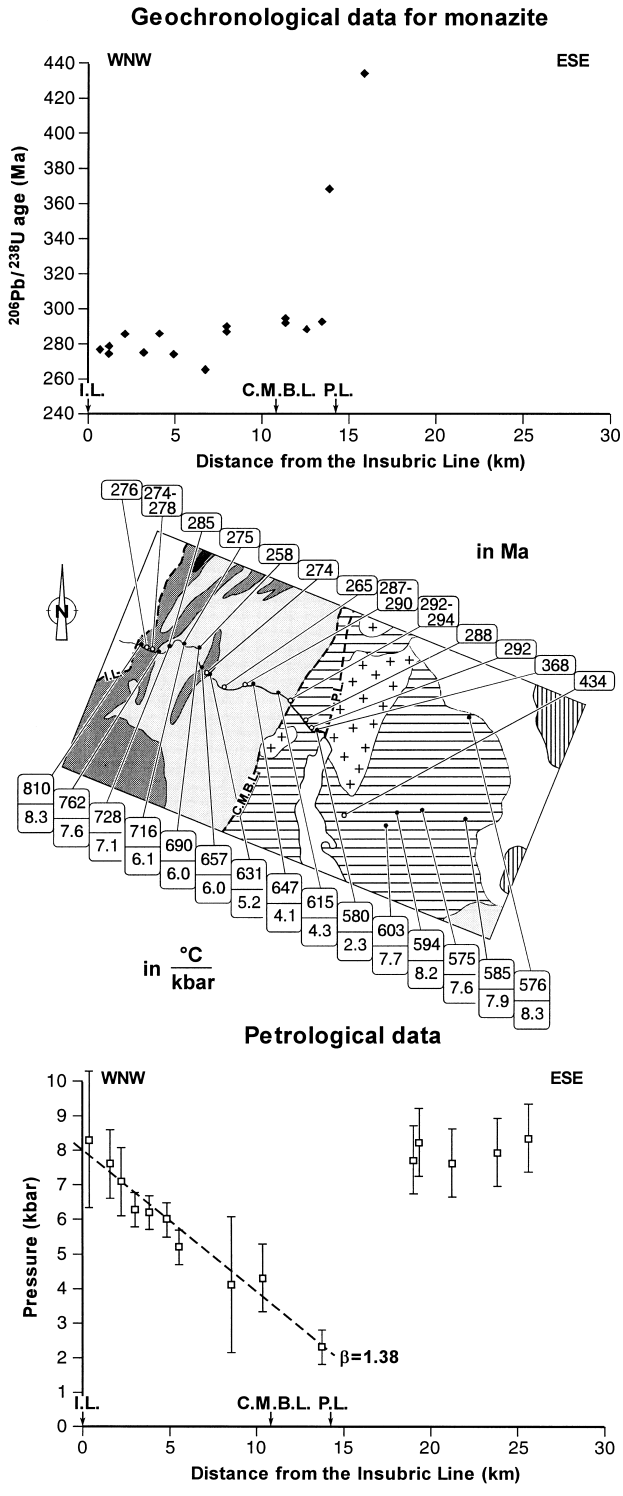

Figure 2. Top—U-Pb age data for monazite (in Ma) and peak metamorphic conditions (bottom, in °C and kbar) along Val Strona traverse. The monazite U-Pb age of 434 Ma is from Köppel and Grünfelder (1971) and was projected into the profile.

Table 1. Peak Metamorphic Conditions for Val Strona Rocks

Sample[a]	Distance from Insubric Line (km)	Rock type	Mineral assemblage	Peak metamorphic conditions		Thermobarometry applied
				T(°C)	P(kbar)	
IZ-93-60	.4	Metagabbro	Grt-Cpx-Pl-Hbl ± Opx, Bt, Rt, Ilm	810 ± 50	8.3 ± 2.0	TWEEQ (1)
IZ-93-61	1.6	Grt-Opx-gneiss	Grt-Opx-Pl-Qtz ± Kfs, Bt, Rt, Ilm	762 ± 30	7.6 ± 1.0	Grt-Opx-thermometry (2) Grt-Opx-Pl-Qtz-barom (2)
IZ-93-63	2.2	Grt-Opx-gneiss	Grt-Opx-Pl-Qtz ± Kfs, Bt, Rt, Ilm	728 ± 30	7.1 ± 1.0	Grt-Opx-thermometry (2) Grt-Opx-Pl-Qtz-barom (2)
VS 30	3.0	Grt-Opx-gneiss	Grt-Opx-Pl-Qtz ± Cum, Bt, Ilm	716 ± 30	6.3 ± 1.0	Grt-Opx-thermometry (2) Grt-Opx-Pl-Qtz-barom (2)
VST 20	3.8	Grt-migmatite	Grt-Sil-Bt-Pl-Kfs-Qtz ± Ilm	690 ± 30	6.0 ± 0.5	Grt-Bt-thermometry (3) GASP-barometry (4)
IZ-93-65	4.8	Grt-Sil-gneiss	Grt-Sil-Bt-Pl-Kfs-Qtz ± Ilm	657 ± 30	6.0 ± 0.5	Grt-Bt-thermometry (3) GASP-barometry (4)
IZ-93-68	5.5	Grt-amphibilite	Grt-Hbl-Pl-Bt ± Ilm, Spn	631 ± 30	5.2 ± 0.5	Grt-Hbl-thermometry (5) Grt-Hbl-Pl-Qtz-barom (6)
IZ-93-100	8.5	Calcsilicate schist	Grt-Cpx-Hbl-Pl-Cal-Qtz ± Bt, Ilm, Spn	647 ± 50	4.1 ± 2.0	Grt-Cpx-thermometry (7) Grt-Cpx-Pl-Qtz-barom (8)
VST 9	10.3	Grt-micaschist	Grt-Bt-Ms-Pl-Qtz ± Ilm	615 ± 30	4.3 ± 1.0	Grt-Bt-thermometry (9) Grt-Pl-Bt-Ms-barom (10)
IZ-93-70	13.7	Sil-And-gneiss	And-Sil-Bt-Ms-Pl-Kfs-Qtz ± Crd, Ilm	580 ± 30	2.3 ± 1.0	Feldspar-thermometry (11) Ms-barometry (12)

Sources. (1) Berman 1991; (2) Lal 1993; (3) Zhu and Sverjensky (1992); (4) Koziol and Newton 1988; (5) Graham and Powell 1986; (6) Kohn and Spear 1990; (7) Ellis and Green 1979; (8) Newton and Perkins 1986; (9) Williams and Grambling 1992; (10) Hoisch 1990; (11) Fuhrman and Lindsley 1988; (12) Massonne 1990.

[a] See figure 2 for sample location.

mated using the Grt-Cpx-Plg-Qtz-geobarometer of Newton and Perkins (1982) or its recalibration by Powell and Holland (1988). Minimum pressures of about 7 kbar are constrained by the transition from basalt to garnet granulite (Ito and Kennedy 1979). A P-T-estimate for the mineral reactions between the silicates, rutile and ilmenite with the TWEEQ-program (Berman 1991) yields 810°C at 8.3 kbar, well within the constrained P-T-box. Decreasing XMg-values toward the rim of the garnet and increasing Al-contents toward the rim of the orthopyroxene indicate cooling to 720 ± 30°C during about 1 kbar decompression.

Toward the southeast a continuous decrease of peak metamorphic conditions can be observed. Granulite facies conditions of 720–760°C at 6.0–8.0 kbar are revealed by the garnet-orthopyroxene-plagioclase-quartz thermobarometry of Lal (1993). Inclusions in garnet and zonation patterns of garnet, orthopyroxene, and plagioclase indicate isobaric cooling processes toward the garnet rim. In higher amphibolite-facies metapelites, the distinct increase in biotite at the expense of garnet is due to the reaction of Grt + Kfs + H_2O <===> Bt + Sil + Qz (Schmid and Wood 1978). Due to high Ti- and F-contents in biotite, the garnet-biotite thermometry of Zhu and Sverjensky (1992) with Margules parameters of Sengupta et al. (1990) was applied to determine metamorphic temperatures, while pressures were estimated with the GASP-calibration of Koziol and Newton (1988). Peak metamorphic conditions within the anatectic zone as revealed by syndeformative biotite and plagioclase-inclusions in the garnet cores of a garnet-sillimanite-mica schist (sample VST 20) are 690 ± 30°C and 6.0 ± 0.5 kbar.

Compositional zoning in garnets, i.e., bell-shaped patterns of Mn and Ca as well as increasing XMg values from core to rim, is present in garnet-amphibolites from the central part of the Val Strona. Mineral thermobarometry yields peak metamorphic conditions of about 630°C and 5.2 kbar using inclusions in the outer core of the garnet. Rim compositions of garnet, hornblende, and plagioclase indicate cooling and a weak decrease in pressure. The first appearance of syndeformative muscovite is recorded in garnet mica schists from the lower part of the Val Strona (sample VST 9). Peak metamorphic conditions are estimated at 615 ± 30°C and 4.3 ± 1 kbar applying garnet-biotite thermometry of Williams and Grambling (1990) and garnet-muscovite-biotite-plagioclase barometry of Hoisch (1990) on garnet inclusions. These estimates are reproduced by garnet-ilmenite barometry (Pownceby et al. 1987*a*, 1987*b*), muscovite barometry of Massonne (1990), and the contoured petrogenetic grid of Spear and Cheney (1989). Matrix minerals and rim composition of the garnet in-

dicate cooling and decompression to 540 ± 30°C and 2.8 ± 1 kbar.

The lowest metamorphic conditions are found within an alumosilicate-bearing gneiss near Omenga (sample IZ-93-70). The coexistence of andalusite and sillimanite, feldspar-thermometry of Fuhrman and Lindsley (1988), and muscovite-barometry (Massonne 1990) point to P-T-conditions of 580 ± 30°C and 2.3 ± 0.5 kbar. As this sample originates already from the SCZ (according to the geological map of Zingg et al. 1990), no significant change in metamorphic pressure can be observed at the CMBL. This could have important consequences for the interpretation of the CMBL (cf. Boriani et al. 1990*a;* Schmid 1993), but more petrologic data are required to place further constraints on the movement history of this fault. Farther to the east, peak metamorphic pressures increase abruptly to about 8 kbar, whereas temperatures remain below 600°C (Franz unpub. data). These data are interpreted as remnants of the earlier tectonometamorphic evolution, possibly related to an early Paleozoic pressure-dominated metamorphic event (see below).

Geochronology. For geochronological investigations, 12 samples of metasedimentary rocks were collected along the Val Strona. Information on the cooling history of the IVZ immediately after high temperature metamorphism is provided by U-Pb age data on monazites (table 2; figure 2, top). The IVZ monazites are unzoned; most show an alignment in the metamorphic foliation. They show generally concordant ages, the oldest age of yield 292 ± 2 Ma recorded near the PL (figure 3; see also data depository for details). With increasing distance from the PL and depth, respectively, ages become systematically younger and finally yield 276 ± 2 Ma at the base of the IVZ. These data illustrate migration of the isotherm equivalent to the monazite closure temperature and progressive cooling of the lower crust after magmatism and crustal attenuation. A closure temperature for U-Pb in monazite from metasedimentary rocks of 600 ± 50°C is assumed (Teufel 1988; Smith and Barreiro 1990).

In contrast to the IVZ, U-Pb ages on monazites and zircons from the SCZ point to an early Paleozoic event of about 450 Ma (Köppel und Gruenfelder 1971; Köppel 1974; Ragettli et al. 1994). This is also supported by our U-Pb age data on zircons from the Ceneri orthogneiss. Seven fractions of long prismatic zircons (sample IZ-94-70) were analyzed (table 2). The larger sieve fractions frequently show rounded inclusions of zircons in the core, which may have been detrital relics from the precursor sediments. The U-Pb data points are discordant in the concordia diagram and scatter around a regression line with an upper and lower intercept corresponding to ages of 2232 ± 65 Ma and 457 ± 9 Ma, respectively. While the 2.23 Ga age is interpreted as an inherited age of the rounded zircon inclusions, the 457 Ma event probably represents the intrusion age of the granitoid protolith of the Ceneri gneiss.

U-Pb age dating of monazite from the same sample (sample IZ-94-70) yields an age of about 370 Ma (figure 2, top; see also Köppel and Grünfelder 1978/79). The age of these slightly discordant monazites seems to be partly rejuvenated by incomplete resetting of the U-Pb system—most likely, because the thermal impact of late Paleozoic magmatic underplating at upper crustal levels was limited.

Crustal Attenuation. Our petrologic data from the IVZ show a correlation of peak metamorphic pressure with distance along surface (= depth) that exceeds the lithostatic gradient of 0.3 kbar/km (Burke and Fountain 1990). The average gradient is about 0.41 kbar/km, suggesting significant crustal thinning, particularly in the lowermost 5 km of the crust, after the mineral barometers were set. Thus, a minimum stretching factor of $\beta = 1.38$ can be inferred from the petrologic data (figure 2, bottom). Similar observations were reported by Sills (1984) who described a pressure gradient of about 0.5 kbar/km within the granulite facies part of the IVZ and by Brodie and Rutter (1987) who infer 2 km of lower crustal thinning from mylonitic shear zones in the lowermost 5 km of the IVZ.

Our P-T estimates from zoning in garnets indicate about 1.3 kbar decompression during retrograde evolution of the IVZ. This is a minimum estimate, as mineral thermometry and barometry probably document only part of the exhumation history. Geochronological and petrologic data strongly suggest that the equivalent 4 km of crustal thinning are Early Permian in age, i.e., before 280–290 Ma, because decompression occurred after high-temperature metamorphism induced by the mafic intrusions but at temperatures still above monazite U-Pb closure temperatures.

Assuming an initial crustal thickness of 30 km, the stretching factor of $\beta = 1.38$ leads to a final crustal thickness of 21 km. Thus, about 4 km of crustal thinning occurred during Early Permian crustal attenuation, while the remaining 5 km may be related to the early Mesozoic rifting event. The inferred amount and timing of crustal attenuation agrees with estimates of Handy (1987) who suggests that faulting at the PL was responsible for about 3 km of crustal thinning sometime between the Early Permian and Middle Triassic and for about 5 km

Table 2. U-Pb Age Data for Monazites and Zircons from the Val Strona

Sample/ Mineral	Distance from the Insubric Line (km)	Sieve fraction (μm)	Measured ratios			Concentrations		Calculated ratios			Apparent ages (Ma)		
			208Pb/206Pb	207Pb/206Pb	206Pb/204Pb	U (ppm)	Pb (ppm)	206Pb/238U	207Pb/235U	207Pb/206Pb	206Pb/238U	207Pb/235U	207Pb/206Pb
VS19													
Mnz	.8	40–160	6.05365	.06685	964.8	2330.0	641.8	.04381	.31202	.05117	276.4	275.8	269.9
VST 21													
Mnz	1.3	40–160	5.81263	.05547	4151.4	2604.0	675.2	.04343	.31102	.05194	274.0	275.0	282.9
Mnz		40–160	5.82533	.05824	2152.8	2353.0	622.6	.04412	.31299	.05145	278.3	276.5	261.1
VST 22													
Mnz	2.2	<60	4.00680	.08201	488.4	3167.0	655.4	.04521	.32415	.052	285.1	285.1	285.4
Mnz		60–100	6.08204	.08283	476.7	2227.0	649.7	.0452	.32468	.0521	285.0	285.5	289.6
VST 4													
Mnz	3.3	40–160	8.42784	.05668	2570.3	1942.0	699.3	.0435	.30574	.05097	274.5	270.9	239.5
VST 20													
Mnz	3.8	40–160	5.07734	.12271	205.8	2950.0	786.6	.04527	.32109	.05144	285.4	282.7	260.8
VST 24													
Mnz	5.0	40–160	4.47876	.05551	4239.1	2928.0	610.4	.04336	.31126	.05206	273.7	275.2	288.0
VST 3													
Mnz	6.8	40–160	1.72183	.06507	1090.2	6991.0	718.2	.04193	.29843	.05162	264.8	265.2	268.6
VST 15													
Mnz	8.0	<60	2.25086	.06013	1818.2	5560.0	732.2	.04553	.32688	.05207	287.0	287.2	288.6
Mnz		60–100	2.50537	.06091	1648.5	5023.0	716.5	.04573	.328	.05202	288.2	288.0	286.4
Mnz		>100	2.83353	.06228	1442.0	4437.0	695.4	.04591	.32992	.05212	289.4	289.5	290.6
Mnz		>100	2.83461	.06227	1452.5	4423.0	694.2	.04596	.33068	.05218	289.7	290.1	293.3
VST 7													
Mnz	11.4	60–100	1.67360	.05542	4492.2	6829.0	754.6	.04666	.33557	.05216	294.0	293.8	292.5
Mnz		>100	1.71556	.05660	3394.5	6915.0	772.2	.04636	.33417	.05228	292.1	292.7	297.8
VST 13													
Mnz	12.6	60–100	1.30151	.06858	895.3	7515.0	717.8	.04569	.32895	.05222	288.0	288.8	295.0
VST 5													
Mnz	13.5	40–160	2.90576	.05520	4853.3	6005.0	958.1	.05219	.3337	.05219	292.2	292.4	293.5
IZ-94-70													
Mnz	13.9	40–160	2.31048	.05949	3030.3	5327.0	918.9	.05883	.4434	.05467	368.5	372.7	398.6
Zrn		<40	.09157	.07690	3656.7	727.4	64.6	.08797	.8854	.07299	543.6	643.9	1013.8
Zrn		<63	.08972	.08133	3298.6	665.5	62.4	.09261	.9835	.07702	570.9	695.4	1121.8
Zrn		<80	.08794	.08217	48796.3	608.5	59.6	.09731	1.0986	.08188	598.6	752.7	1242.6
Zrn		<102	.08940	.08514	5386.1	472.3	56.3	.11766	1.3388	.08252	717.1	862.7	1258.0
Zrn		<125	.09527	.09007	5112.1	684.8	74.3	.10606	1.2771	.08733	649.8	835.6	1367.8
Zrn		<160	.09382	.09436	3427.4	432.4	60.5	.13615	1.6949	.09029	822.9	1006.6	1431.6
Zrn		<200	.10081	.10325	4072.8	562.5	67.0	.11451	1.5766	.09986	698.9	961.0	1621.5

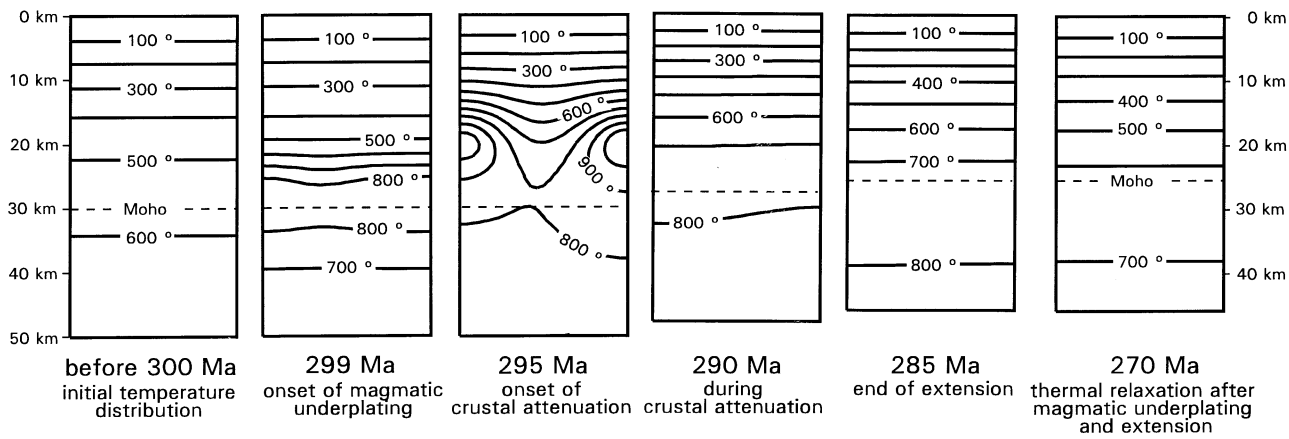

Figure 3. Evolution of the lithospheric temperature field during and after magmatic underplating and crustal attenuation.

during the Late Triassic to Middle Jurassic, leaving a crust of approximately 20 km thickness.

Timing of Magmatic Underplating, Metamorphism, and Crustal Attenuation. The timing of magmatic underplating, metamorphism, and crustal attenuation can be constrained by various lines of evidence. Our monazite data suggest that magmatic underplating started a few myr before 292 ± 2 Ma, because this age already reflects cooling after the thermal front induced by the mafic intrusions had reached the intermediate crust. In the lowermost crust, the lower intercept zircon age indicates granulite-facies metamorphism at 285 ± 10 Ma (Köppel 1974). The end of penetrative deformation is marked by the emplacement of the uppermost, undeformed parts of the Mafic Formation at 285 +7/−5 Ma (Pin 1986), which is also interpreted as a late intrusion with respect to regional metamorphism (Zingg et al. 1990). Quick et al. (1994) describe synmagmatic deformation of the Mafic Formation, which they relate to crustal extension. We did not find any P-T paths documenting crustal heating during decompression, which could be expected if extension triggered melt generation. Instead, the thermobarometric data only indicate cooling during exhumation. This may suggest that magmatic underplating at least enhanced crustal attenuation—rather than being a consequence of it—as the addition of heat and low-viscosity material certainly reduced the crustal strength. From the available data we therefore infer that magmatic underplating culminated between about 300 and 295 Ma. It was partly contemporaneous, but essentially followed by, crustal extension lasting until about 285 Ma. At shallower crustal levels with an earlier cooling history, generally undeformed dioritic and granitic intrusions ranging between 290 and 270 Ma clearly postdate the thermal peak of metamorphism (Zingg et al. 1990).

Thermal Modeling Approach

Calculation of the crustal temperature field and its change with time are based on a thermal-kinematic modeling approach. Finite element techniques are used to model time-dependent heat transfer by conduction and advection during magma intrusion and crustal extension (i.e., Carslaw and Jaeger 1959; Turcotte and Schubert 1982). As we are interested in the long-term, i.e., subsolidus cooling history of the intrusions, early convective heat transport (Huppert and Sparks 1988) and synmagmatic flow (Quick et al. 1994) within the sills can be neglected. A two-dimensional modeling approach is used to account for the lateral variations in the thickness of the Mafic Formation, particularly in the Val Strona area.

Table 3. Modeling Parameters

Surface temperature	0°C
Specific heat	1300 J Kg^{-1} $°K^{-1}$
Density (Burke and Fountain, 1990):	
upper crust	2700 kg m^{-3}
lower crust	3000 kg m^{-3}
upper mantle	3300 kg m^{-3}
Radiogenic heat production (calc. after Schnetger (1994):	
upper crust	2.30×10^{-6} W m^{-3}
lower crust	1.42×10^{-6} W m^{-3}
upper mantle	0.02×10^{-6} W m^{-3}
Thermal conductivity (W m^{-1} $°K^{-1}$, T in °C) (calc. after Clauser and Huenges 1995)	
upper crust	2.8/(1 + 0.0013 T)
lower crust	3.5/(1 + 0.0012 T)
upper mantle	3.5 (W m^{-1} $°K^{-1}$
Basal heat flow	0.017 W m^{-2}
Basalt (Thompson 1992)	
intrusion temperature	1250 °C
cryst. temperature	1150 °C
latent heat of cryst.	$5 > 10^5$ J kg^{-1}
Crust:	
melting temperature	800 °C
latent heat of fusion	2×10^5 J kg^{-1}

The initial model geometry comprises a 26 km wide and 50 km thick section of the upper lithosphere centered around the Val Strona (box in figure 1). In this area the underplated igneous complex is exceptionally thin, and the Kinzigite Formation reaches its maximum thickness. An initial Moho depth of 30 km (Handy 1987) was chosen, supported by our petrologic data showing pressures equivalent to about 28 km depth near the base of the IVZ. The numerical model is subdivided into three layers—upper crust, lower crust, and upper mantle—with distinct thermal properties (table 3). Temperature-dependent thermal conductivities and the contribution of latent heats of crystallization and fusion to the total heat budget are taken into account.

The crustal temperature field immediately before magmatic underplating is difficult to constrain since the subsequent high-temperature metamorphism essentially erased all information. Regarding the late-orogenic setting, we choose an initial surface heat flow of 70 mW m^{-2}, which results in an initial Moho temperature of about 580°C. Magma intrusions at the base of or into the lower crust are modeled by temporarily setting selected nodes of the finite element grid to a temperature of 1250°C. This procedure is designed to mimic repeated em-

placement of 1 km thick mafic sills. Melt intrusion is modeled as an instantaneous process as magmas ascend much faster than they cool. We assume that intrusions were spread over 5 myr and that the vertical succession of intrusions in the Mafic Formation corresponds also to a temporal order, starting with the oldest intrusion at the base (Voshage et al. 1990). The spatial distribution was selected according to the present occurrence of the Mafic Formation in map view (see box in figure 1; without quartz-dioritic rim) restored to its preextensional position. Thus, the IVZ was thickened homogeneously by a factor of 1.38 to achieve the initial geometry.

As our geochronological data from the IVZ yield only very Late Carboniferous to Early Permian ages, we concentrate on the late Paleozoic extensional episode. The related 4 km of crustal attenuation are modeled by simple shear at the base of the upper crust resembling fault movement at the PL and by pure shear thinning of the lower 18 km of the crust, both perpendicular to the plane of observation. The thermal effects of post-tectonic granites intruding in the vicinity of the PL at 276 ± 5 Ma (Hunziker and Zingg 1980) are not considered, because the related disturbance of the crustal temperature field was only local and remained below the temperatures documented by our geochronological and petrologic data.

Results of Thermal Modeling

Numerical simulation results illustrate the strong disturbance of the crustal temperature field due to magmatic underplating and subsequent thermal relaxation during cooling of the intrusions and crustal extension (figure 3). Repeated magma intrusions spread over 5 myr, i.e., between 300 and 295 Ma, induced regional-scale granulite- to amphibolite-facies metamorphism and anatexis in the lower crust and heated even the top of the lower crust to temperatures of about 600°C. The heat budget is essentially a balance between the heat derived from cooling and crystallization of the basaltic intrusions and the heat required for heating and partial melting of crustal rocks.

The calculated temporal evolution of depth and temperature of single grid points can be compared to our petrologic and geochronological data outlined above. Modeling results can reproduce the observed P-T-paths, particularly the cooling of individual samples during decompression (figure 4). Peak metamorphic temperatures in the crustal column were reached at slightly different times: immediately after the first intrusions, i.e., at 300 Ma, in the lowermost crust, but not before about 295

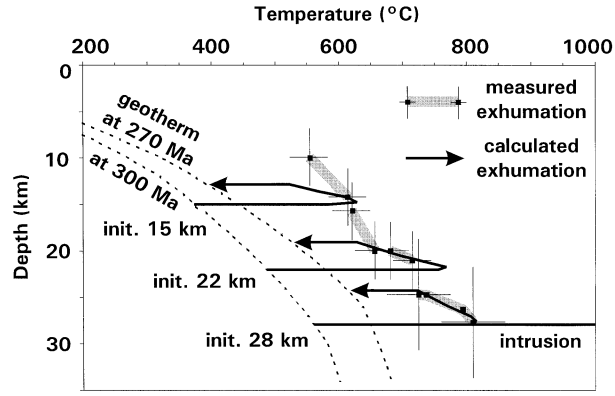

Figure 4. Comparison between observed exhumation paths and modeled P-T evolution of the Ivrea Zone during the Late Paleozoic.

Ma at mid-crustal levels. Thermal modeling predicts that temperatures in the upper part of the IVZ dropped below the monazite closure temperature of about 600°C at 294 Ma (figure 5). Thus, at shallower crustal levels, final heating was still contemporaneous with extension, while in the lower parts of the section extension postdates the thermal peak of metamorphism. The numerical simulation indicates that the base of the IVZ passed through the assumed monazite closure temperature of 600°C at about 270 Ma, so that magmatic underplating resulted in elevated lower crustal temperatures for about 30 myr. This thermal event was sufficiently strong to erase essentially all memories of the earlier tectonometamorphic history and to reset mineral chemical and isotopic equilibria in the IVZ. Indications for an earlier baric peak and older age data, which presumably also existed in the IVZ, were only preserved in the SCZ because upper crustal levels were only mildly affected by the mafic intrusions at depth.

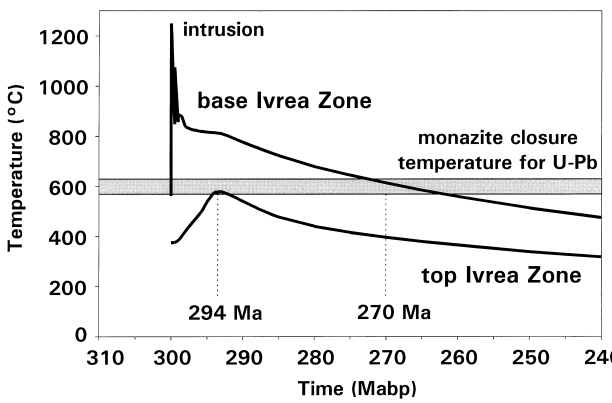

Figure 5. Comparison between observed U-Pb monazite ages from the top and base of the Ivrea Zone and modeled cooling history.

Conclusions

We have shown that the temperature increase caused by magmatic underplating in the IVZ was sufficient to reset mineral chemical and isotopic equilibria in the lower and even intermediate crust. Only in the upper crust memories of the metamorphic evolution pre-dating high-temperature metamorphism at depth had a chance to survive. Modeling results illustrate migration of the heating and cooling fronts through the crust and explain the progressive younging of monazite U-Pb ages toward the Moho. After thermal relaxation a heterogeneous crustal succession is left behind: a pressure-dominated metamorphic upper crust of Ordovician to Silurian age resting on top of a high-temperature late Paleozoic lower crust.

Modeling results document, in general, how even a coherent crustal section can achieve a strongly heterogenous metamorphic grade and isotopic ages through the thermal effects of magmatic underplating and crustal attenuation. In cases of a strongly increased basal heat flow into the crust, e.g., by magmatic underplating, delamination of the mantle lithosphere, etc., it may be very difficult to infer the tectonometamorphic history of the entire crust from the study of exposed crystalline complexes, which usually show only distinct crustal and metamorphic levels.

ACKNOWLEDGMENT

We mourn for our colleague and friend Stefan Teufel. He completed the geochronological work and even a month before his sudden death he was in the Ivrea Zone collecting new samples for age determinations. We are grateful to Mark Handy, George Bergantz, David M. Fountain, Arthur W. Snoke and an anonymous reviewer for their helpful comments on an earlier version of the manuscript.

REFERENCES CITED

Berman, R. G., 1991, Thermobarometry using multiequilibrium calculations: a new technique with petrologic applications: Can. Mineral., v. 29, p. 833–885.

———; Aranovich, L. Y.; and Pattison, D. R. M., 1995, Reassessment of the garnet-clinopyroxene Fe-Mg exchange thermometer: II. Thermodynamic analysis: Contrib. Mineral. Petrol., v. 119, p. 30–42.

Borghi, A., 1988, Evoluzione metamorfica del settore nord-est della Serie del Laghi (Alpi Meriodionalli–Canton Ticiono): Rend. Soc. Geol. Ital., v. 11, p. 165–170.

Boriani, A.; Burlini, L.; and Sacchi, R., 1990*a,* The Cossato-Mergozzo-Brissago line and the Pogallo line (southern Alps, northern Italy) and their relationships with the Late Hercynian magmatic and metamorphic events: Tectonophysics, v. 182, p. 91–102.

———; Giobbi Origoni, E.; Borghi, A.; and Caironi, V., 1990*b,* The evolution of the ''Serie dei Laghi'' (Strona-Ceneri and Schisti dei Laghi): The upper component of the Ivrea-Verbano crustal section; southern Alps, north Italy and Ticino, Switzerland: Tectonophysics, v. 182, p. 103–118.

Brodie, K. H.; Rex, D.; and Rutter, E. H., 1989, On the age of deep crustal faulting in the Ivrea zone, northern Italy, *in* Coward, M. P.; Dietrich, D.; and Park, R. G., eds., Alpine tectonics: Geol. Soc. (London) Spec. Pub. 45, p. 203–210.

———, and Rutter, E. H., 1987, Deep crustal extensional faulting in the Ivrea zone of northern Italy: Tectonophysics, v. 140, p. 193–212.

Burke, M. M., and Fountain, D. M., 1990, Seismic properties of rocks from an exposure of extendend continental crust—new laboratory measurements from the Ivrea Zone: Tectonophysics, v. 182, p. 119–146.

Carslaw, H. S., and Jaeger, J. C., 1959, Conduction of Heat in Solids: Oxford, Oxford University Press, 510 p.

Clauser, C., and Huenges, E., 1995, Thermal conductivity of rocks and minerals, *in* Ahrens, T. J., ed., Rock physics and phase relations: A handbook of physical constants: Washington, Am. Geophys. Union, p. 105–126.

Ellis, D. H., and Green, E. H., 1979, An experimental study of the effect of Ca upon garnet-clinopyroxene Fe-Mg exchange equilibria: Contrib. Mineral. Petrol., v. 71, p. 13–22.

Fountain, D. M., 1989, Growth and modification of lower continental crust in extended terrains: The role of extension and magmatic underplating, *in* Mereu, R. F., et al., eds., Properties and processes of earth's lower crust: Am. Geophys. Union Mon. 51, p. 287–299.

Fuhrman, M. L., and Lindsley, D. H., 1988, Ternary feldspar modeling and thermometry: Am. Mineral., v. 73, p. 201–215.

Graham, C. M., and Powell, R., 1986, A garnet-hornblende geothermometer: Calibration, testing, and application to the Pelona schists, southern California: Jour. Meta. Geol., v. 2, p. 13–31.

Handy, M. R., 1987, The structure, age, and kinematics of the Pogallo Fault zone, southern Alps, northwestern Italy: Eclogae Geol. Helvetiae, v. 80, p. 593–632.

———, and Zingg, A., 1991, The tectonic and rheological evolution of an attenuated cross section of the continental crust: Ivrea crustal section, southern Alps, northwestern Italy, and southern Switzerland: Geol. Soc. America Bull., v. 103, p. 236–253.

Hodges, K. V., and Fountain, D. M., 1984, The Pogallo line, south Alps, northern Italy: An intermediate crustal level, low-angle normal fault?: Geology, v. 12, p. 151–155.

Hoisch, T. D., 1990, Empirical calibration of six geobarometers for the mineral paragenesis quartz + muscovite + biotite + plagioclase + garnet: Contrib. Mineral. Petrol., v. 104, p. 225–234.

Hunziker, J. C., and Zingg, A., 1980, Lower Paleozoic amphibolite to granulite facies metamorphism in the Ivrea zone (southern Alps, northern Italy): Schweizer Mineral. Petrograph. Mitteilungen, v. 60, p. 181–213.

Huppert, H. E., and Sparks, S. J., 1988, The generation of granitic magmas by intrusion of basalt into continental crust: Jour. Petrol., v. 29, p. 599–624.

Ito, K., and Kennedy, G. C., 1979, An experimental study of the basalt-garnet granulite-eclogite transition, *in* Heacock, J. G., ed., The structure and physical properties of the earth's crust: Am. Geophys. Union Mon. 14, p. 303–314.

Köppel, V., 1974, Isotopic U-Pb ages of monazites and zircons from the crust-mantle transition and adjacent units of the Ivrea and Ceneri Zones (southern Alps, Italy): Contrib. Mineral. Petrol., v. 43, p. 55–70.

———, and Grünfelder, M., 1971, A study of inherited and newly formed zircons from paragneisses and granitised sediments of the Strona-Ceneri-Zone (southern Alps): Schweizer mineral. petrogr. Mitteilungen, v. 51, p. 385–410.

———, and ———, 1978/1979, Monazite and zircon U-Pb ages from the Ivrea and Ceneri zones; *in* Abstr., 2nd Sym. Ivrea-Verbano, Varallo: Mem. Sci. Geol. Padova, v. 33, p. 257.

Kohn, M., and Spear, F. S., 1990, Two new geobarometers for garnet amphibolites, with applications to southeast Vermont: Am. Mineral., v. 75, p. 89–96.

Koziol, A. M., and Newton, R. C., 1988, Redetermination of the anorthite breakdown reaction and improvement of the plagioclase-garnet-Al_2SiO_5-quartz geobarometer: Am. Mineral., v. 73, p. 216–223.

Kretz, R., 1983, Symbols for rock-forming minerals: Am. Mineral., v. 68, p. 277–279.

Lal, R. K., 1993, Internally consistent recalibrations of mineral equilibria for geothermobarometry involving garnet-orthopyroxene-plagioclase-quartz assemblages and their application to the south Indian granulites: Jour. Meta. Geol., v. 11, p. 855–866.

Mareschal, J.-C., and Bergantz, J., 1990, Constraints on thermal models of the Basin and Range province: Tectonophysics, v. 174, p. 137–146.

Massonne, H.-J., 1990, High-pressure, low-temperature metamorphism of pelitic and other protoliths based on experiments in the system K_2O-MgO-Al_2O_3-SiO_2-H_2O: Habilitation thesis, Ruhr Universität, Bochum, Germany, 172 p.

Newton, R. C., and Perkins, D. III, 1982, Thermodynamic calibration of geobarometers based on the assemblages garnet-plagioclase-orthopyroxene (clinopyroxene)-quartz: Am. Mineral., v. 67, p. 203–222.

Pin, C., 1986, Datation U-Pb sur zircons a 285 Ma du complexe gabbro-dioritique du Val Sesia–Val Mastallone etage tardi-hercynien du métamorphisme granulitique de la zone Ivrea-Verbano (Italie): C.R. Acad. Sci. Paris, v. 303/II, p. 827–830.

Powell, R., and Holland, T. J. B., 1988, An internally consistent dataset with uncertainties and correlations: 3. Applications to geobarometry, worked examples and a computer program: Jour. Meta. Geol., v. 6, p. 173–204.

Pownceby, M. I.; Wall, V. J.; and O'Neill, H. S. C., 1987*a*, Fe-Mn partitioning between garnet and ilmenite: Experimental calibration and applications: Contrib. Mineral. Petrol., v. 97, p. 116–126.

———; ———; and ———, 1987*b*, Fe-Mn partitioning between garnet and ilmenite: experimental calibration and applications (correction): Contrib. Mineral. Petrol., v. 97, p. 539.

Quick, J. E.; Sinigoi, S.; and Mayer, A., 1994, Emplacement dynamics of a large mafic intrusion in the lower crust, Ivrea-Verbano Zone, northern Italy: Jour. Geophys. Res., v. 99, p. 21,559–21,573.

Ragettli, A. R.; Hebeda, E. H.; Signer, P.; and Wieler, R., 1994, Uranium-xenon chronology: precise determination of λ_{sf}. $^{136}Y_{sf}$. for spontaneous fission of ^{238}U: Earth Planet. Sci. Lett., v. 128, p. 653–670.

Schnetger, B., 1994, Partial melting during the evolution of the amphibolite- to granulite-facies gneisses of the Ivrea Zone, northern Italy: Chem. Geol., v. 113, p. 71–101.

Schmid, R., and Wood, B. J., 1978, Phase relationshis in granulitic metapelites from the Ivrea-Verbano Zone (northern Italy): Contrib. Mineral. Petrol., v. 54, p. 255–279.

Schmid, S. M., 1993, Ivrea Zone and adjacent Southern Alpine Basement, *in* v. Raumer, J. F., and Neubauer, F., eds., Pre-Mesozoic Geology in the Alps: Berlin, Springer-Verlag, p. 567–583.

Sengupta, B.; Bhattacharia, P. K.; and Mukherjee, M. 1990, An orthopyroxene-biotite geothermometer and its application in crustal granulite and mantle-derived rocks: Jour. Meta. Geol., v. 8, p. 191–197.

Sills, J. D., 1984, Granulite facies metamorphism in the Ivrea zone, NW Italy: Schweizer Mineral. Petrograph. Mitteilungen, v. 64, p. 169–191.

Sinigoi, S.; Quick, J. E.; Clemens-Knott, D.; Mayer, A.; Demarchi, G.; Mazzucchelli, M.; Negrini, L.; and Rivalenti, G., 1994, Chemical evolution of a large mafic intrusion in the lower crust, Ivrea-Verbano Zone, northern Italy: Jour. Geophys. Res., v. 99, p. 21,575–21,590.

Smith, H. A., and Barreiro, B., 1990, Monazite U-Pb dating of staurolite-grade metamorphism in pelitic schists: Contrib. Mineral. Petrol., v. 105, p. 602–615.

Spear, F. S., and Cheney, J. T., 1989, A petrogenetic grid for pelitic schists in the system SiO_2-Al_2O_3-FeO-MgO-K_2O-H_2O: Contrib. Mineral. Petrol., v. 101, p. 149–164.

Strackenbrock-Gehrke, I., 1989, Thermometrie und Graphitgenese in Metakarbonaten der Ivrea-Zone (Norditalien): Unpub. Ph.D. thesis, Universität Göttingen, Germany, 120 p.

Teufel, S., 1988, Vergleichende U-Pb- und Rb-Sr-Altersbestimmungen an Gesteinen des Übergangsbereiches Saxothuringikum/Moldanubikum, NE-Bayern: Göt-

tinger Arbeiten zur Geologie und Paläontologie v. 35, 87 p.

Thompson, A. B., 1992, Metamorphism and Fluids, *in* Brown, G. C.; Hawkesworth, C. J.; and Wilson, R. C. L., eds., Understanding the Earth: Cambridge, Cambridge University Press, p. 222–248.

Turcotte, D. L., and Schubert, G., 1982, Geodynamics: Wiley, New York, 450 p.

Vavra, G.; Gebauer, D.; Schmid, R.; and Compston, W., 1996, Multiple zircon growth and recrystallisation during polyphase Late Carboniferous to Triassic metamorphism in granulites of the Ivrea Zone (southern Alps): an ion microprobe (SHRIMP) study: Contrib. Mineral. Petrol., v. 122, p. 337–358.

Voshage, H.; Hofmann, A. W.; Mazzucchelli, M.; Rivalenti, G.; Sinigoi, S.; Raczek, I.; and Demarchi, G., 1990, Isotopic evidence from the Ivrea Zone for a hybrid lower crust formed by magmatic underplating: Nature, v. 347, p. 731–736.

———; Hunziker, J. C.; Hofmann, A. W.; and Zingg, A., 1987, A Nd and Sr isotopic study of the Ivrea zone, southern Alps, N-Italy: Contrib. Mineral. Petrol., v. 97, p. 31–42.

Williams, M. L., and Grambling, J. A., 1990, Manganese, ferric iron, and the equilibrium between garnet and biotite: Am. Mineral. v. 75, p. 886–908.

Zhu, C., and Sverjensky, D. A., 1992, F-Cl-OH partitioning between biotite and apatite: Geochim. Cosmochim. Acta, v. 56, p. 3435–3467.

Zingg, A.; Handy, M. R.; Hunziker, J. C.; and Schmid, S. M., 1990, Tectonometamorphic history of the Ivrea Zone and its relationships to the crustal evolution of the Southern Alps: Tectonophysics, v. 182, p. 169–192.